frontiers in Chemistry

ORIGINAL RESEARCH
published: 14 June 2019
doi: 10.3389/fchem.2019.00443

Enhanced Activity and Stability of Gold/Ceria-Titania for the Low-Temperature Water-Gas Shift Reaction

James H. Carter[1], Parag M. Shah[1], Ewa Nowicka[1], Simon J. Freakley[2], David J. Morgan[1], Stan Golunski[1] and Graham J. Hutchings[1]**

[1] School of Chemistry, Cardiff Catalysis Institute, Cardiff University, Cardiff, United Kingdom, [2] Department of Chemistry, Bath University, Bath, United Kingdom

Gold supported on ceria-zirconia is one of the most active low temperature water-gas shift catalysts reported to date but rapid deactivation occurs under reaction conditions. In this study, ceria-titania was evaluated as an alternative catalyst support. Materials of different Ce:Ti compositions were synthesized using a sol-gel methodology and gold was supported onto these using a deposition-precipitation method. They were then investigated as catalysts for the low-temperature water-gas shift reaction. $Au/Ce_{0.2}Ti_{0.8}O_2$ exhibited superior activity and stability to a highly active, previously reported gold catalyst supported on ceria-zirconia. High activity and stability was found to be related to the support comprising a high number of oxygen defect sites and a high specific surface area. These properties were conducive to forming a highly active catalyst with well-dispersed Au species.

Keywords: water-gas shift, gold, ceria-titania, ceria-zirconia, heterogeneous catalysis, nanoparticles

OPEN ACCESS

Edited by:
Svetlana Ivanova, Universidad de Sevilla, Spain

Reviewed by:
Tatyana Todorova Tabakova, Institute of Catalysis (BAS), Bulgaria
Laura Pastor Perez, University of Alicante, Spain

****Correspondence:***
James H. Carter
carterj5@cardiff.ac.uk
Graham J. Hutchings
hutch@cardiff.ac.uk

Specialty section:
This article was submitted to Catalysis and Photocatalysis, a section of the journal Frontiers in Chemistry

Received: *08 May 2019*
Accepted: *29 May 2019*
Published: *14 June 2019*

Citation:
Carter JH, Shah PM, Nowicka E, Freakley SJ, Morgan DJ, Golunski S and Hutchings GJ (2019) Enhanced Activity and Stability of Gold/Ceria-Titania for the Low-Temperature Water-Gas Shift Reaction. Front. Chem. 7:443. doi: 10.3389/fchem.2019.00443

INTRODUCTION

The low-temperature water-gas shift (LTS) reaction has been extensively studied in recent years as a means of upgrading reformate by removing CO and generating H2 (Fu et al., 2003; Tibiletti et al., 2005; Reina et al., 2014). For this application, the catalyst must be both highly active and stable over long times on-stream. Current industrial catalysts based on CuZnO lack the requisite intrinsic activity at lower temperatures and this has prompted the search for new higher activity catalysts.

Au/CeO_2 was initially reported to be highly active for the LTS reaction (Fu et al., 2001) and more recently Hardacre et al. demonstrated that the addition of Zr to the CeO_2 support resulted in a remarkable enhancement of catalyst activity (Tibiletti et al., 2005). However, these gold-based catalysts are unstable under reaction conditions. Goguet et al. reported that the deactivation mechanism of $Au/Ce_{0.5}Zr_{0.5}O_2$ involved a change in the morphology of the gold nanoparticle whereby the effective length of the metal-support interface, the proposed active sites, was reduced as the gold nanoparticle de-wetted (Goguet et al., 2007). We recently showed using stop-start HAADF STEM and XPS that in addition to morphological changes, particle agglomeration also occurs under comparable LTS reaction conditions at 150°C (Carter et al., 2017). The consensus is that the underlying cause of catalyst deactivation is due to a weak interaction between supported gold nanoparticles and cerium oxide-based supports.

It has been reported that defect sites in CeO_2 can function as nucleation sites for Au and stabilize small nanoparticles of gold (Burch et al., 2010; Pojanavaraphan et al., 2013; Laguna et al., 2015). Therefore, a possible strategy to stabilize the supported Au catalyst is to synthesize a support with a high concentration of defects; one such candidate is ceria-titania. Although not as widely studied as ceria-zirconia, it has been investigated as a catalyst support for applications such as CO oxidation (Rodriguez et al., 2015; Rico-Francés et al., 2016) and dry methane reforming (Kim et al., 2015). In a similar way to ceria-zirconia, the addition of Ti to CeO_2 gives enhanced redox properties. It should be noted that Au/TiO_2 is not active for the LTS reaction due to the low concentration of defect sites that facilitate water activation; hence the inclusion of Ce in the many of the most active reported LTS catalysts. One of the earliest examples of ceria-titania being used as a mixed metal oxide support was by Mastelaro et al. who supported CuO on ceria-titania and reported an improvement in catalytic activity for methanol oxidation (Francisco et al., 2001). The reasoning for this was partly ascribed to the enhancement in the textural properties of the materials. Compared with the TiO_2-only sample, the surface area of the mixed metal oxide increased while the crystallite size decreased. Manzoli et al. compared the catalytic activity of Au/CeO_2, Au/TiO_2, $Au/Ce_{0.5}Ti_{0.5}O_2$, and $Au/Ce_{0.2}Ti_{0.8}O_2$ for the low-temperature water-gas shift reaction under an idealized gas composition i.e., in the presence of just CO and H_2O (Manzoli et al., 2007). It was shown that $Au/Ce_{0.2}Ti_{0.8}O_2$ was the most active catalyst. Although this work highlighted the potential of ceria-titania as a support for LTS catalysts, the on-stream stability was not measured. Interestingly, Au/TiO_2 was found to be more active than Au/CeO_2 in contrast to other reports that did not observe LTS activity in Au/TiO_2 below 350°C (Tibiletti et al., 2005). The difference in catalyst preparation or reaction conditions could have contributed to the discrepancies observed in the catalyst activity between these two reports.

Rodriguez et al. have made significant contributions to understanding the fundamental processes that occur in the LTS reaction using gold supported on CeO_2/TiO_2 as model catalysts. Recently they showed that $Au/CeO_x/TiO_2(110)$ was remarkably active for LTS (Park et al., 2009). The activity of this system was markedly higher than the activity of gold supported on CeO2(111) or $Au/TiO_2(110)$. It was shown using a combination of density functional theory and X-ray photoelectron spectroscopy (XPS) that the Ce^{3+} cation is stabilized on $CeO_x/TiO_2(110)$, leading to high activity. Rodriguez et al. also demonstrated the high activity of this support can be observed when other metals such as copper and platinum were deposited (Park et al., 2010).

In this work, a series of catalysts consisting of gold supported on a range of ceria-titanias were prepared, characterized, and investigated for the LTS reaction and compared to $Au/Ce_{0.5}Zr_{0.5}O_2$ as well as CeO_2. The textural and chemical properties were probed to gain an understanding of the trends in catalytic activity and stability and how these relate to the catalyst structure.

EXPERIMENTAL

The $Ce_{1-x}Ti_xO_2$ supports were prepared using a sol-gel methodology previously reported (Rynkowski et al., 2000). The desired ratio of $Ce(NO_3)_3{\cdot}6H_2O$ (Sigma Aldrich, 99.99%) and $Ti[OCH(CH_3)_2]_4$ (Sigma Aldrich, >97%) were dissolved in ethanol (150 cm^3) at room temperature such that the total moles of metal in solution was 0.02. NH_4OH (2 M, Fisher Scientific, 28–30 w/w% in H_2O) was then added drop-wise to this solution until pH 9 was attained. The temperature of the reaction mixture was subsequently increased to 75°C for 30 min to remove the ethanol. After the majority of the solvent was removed, the mixture was filtered and the resulting solid was washed with deionised water (500 cm^3) and dried (110°C, 16 h). The resulting powder was ground using a mortar and pestle and calcined in flowing air (450°C, 5 h, heating rate 10°C min^{-1}). A range of ceria-titania ($Ce_{1-x}Ti_xO_2$) materials were prepared where $x = 0$, 0.1, 0.2, 0.5, and 0.9.

$Ce_{0.5}Zr_{0.5}O2$ was prepared by a sol-gel method previously reported (Pilasombat et al., 2012). Appropriate molar quantities of $Ce(NO_3)_3{\cdot}6H_2O$ and $ZrO(NO_3)_2{\cdot}xH_2O$ (Sigma Alrich, 99.99%) were added to deionised water (300 cm^3) at 80°C, under vigorous stirring in order to give the desired 1:1 molar ratio of Ce:Zr. Once the metal precursors had dissolved, NH_4OH (0.5 M, Fisher Scientific, 28–30 w/w% in H_2O) was added drop-wise until the pH reached 9. The reaction mixture was then immediately filtered under vacuum and washed with warm distilled water (600 cm^3) before being dried (110°C, 16 h). The resultant solid was ground using a mortar and pestle and then calcined under flowing air at (500°C, 5 h, 10°C min^{-1}).

Gold was deposited onto the supports using the deposition-precipitation method. Typically, the support was added to deionised water (200 cm^3) at 60°C while stirring vigorously. Aqueous $HAuCl_4$ (1.63 ml, 12.25 mg ml^{-1}, Strem, 99.8%) was then added to give a nominal loading of 2 wt%. After 15 min, Na_2CO_3 (0.05 M) was added drop-wise until pH 8.0 was reached. The mixture was then stirred for 1 h before the solid was recovered by filtration under vacuum and washed with warm deionised water (600 cm^3). The catalysts were dried (110°C, 5 h) under static air.

X-ray diffraction patterns were obtained on an X'PertPRO PANalytical instrument using Cu Kα (1.54 Å) radiation and were calibrated against a Si standard. Measurements were taken in the range of $2\theta = 10{-}80^{\circ}$.

Raman spectroscopy was performed on a Renishaw ramascope using a spectrophysics 514 nm HeNe laser (20 mW). Surface area measurements were carried out at −196°C on a Quantachrome Quadrasorb SI instrument after each sample was evacuated for 2 h at 120°C. Brunauer–Emmet–Teller (BET) theory over the range $P/P_0 = 0.05$–0.2 was used to calculate the specific surface area.

Scanning electron microscopy-energy dispersive x-ray spectroscopy (SEM-EDX) measurements were performed on a JEOL 6610LV equipped with an Oxford Instruments energy dispersive X-ray (EDX) analyser. The EDX instrument was calibrated using a Co standard.

XPS was carried out on a Kratos Axis Ultra-DLD XPS spectrometer equipped with an AlKα X-ray 300 W source. A C 1s reference (284.7 eV) was used as a calibration. Peaks were fitted as Gaussian Lorentzian curves GL(30) using CasaXPS software.

The actual Au loadings of the catalysts were determined using an Agilent 4,100 MP-AES spectrometer equipped with a nitrogen plasma. A sample of each catalyst (50 mg) was digested in aqua regia (4 cm^3) at ambient temperature for 16 h, before dilution in deionized water up to a total volume of 25 cm^3. Remaining solids were filtered before analyzing the final solution.

Water-gas shift catalysis was carried out on a custom-made fixed-bed flow reactor at a temperature of 150°C. The catalyst (0.150 g) was suspended between two pieces of glass wool. The gas feed consisted of 2% CO, 2% CO_2, 7.5% H_2O, 8.1% H_2, and N_2 to balance. The total flow rate was 100 ml min^{-1} which corresponds to a GHSV of 52,000 h^{-1}).

TABLE 1 | Textural and chemical properties of the $Ce_xTi_{1-x}O_2$ and $Ce_{0.5}Zr_{0.5}O_2$ catalysts.

Sample	Ce:M molar ratio		Specific surface area[b] (m^2 g^{-1})	Crystallite size[c] (Å)
	Nominal	Actual[a]		
CeO_2	–	–	62	123
$Ce_{0.9}Ti_{0.1}O_2$	9	10.2	106	51
$Ce_{0.5}Ti_{0.5}O_2$	1	0.94	143	42
$Ce_{0.2}Ti_{0.8}O_2$	0.25	0.23	300	amorphous
$Ce_{0.1}Ti_{0.9}O_2$	0.11	0.11	191	amorphous
$Ce_{0.5}Zr_{0.5}O_2$	1	1.23	83	71

[a] *Elemental composition determined using SEM-EDX.*
[b] *Specific surface area measurements determined using N_2 porosimetry BET method.*
[c] *Crystallite size determined using the Scherrer Equation from XRD patterns of each material.*

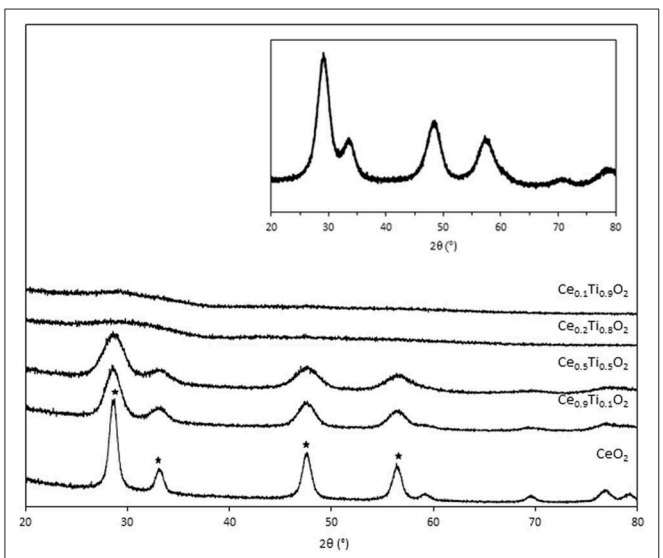

FIGURE 1 | XRD stack of synthesized the $Ce_xTi_{1-x}O_2$ materials, showing cubic fluorite reflection of CeO_2 (*). Inset: XRD pattern of $Ce_{0.5}Zr_{0.5}O_2$.

RESULTS AND DISCUSSION

Initially, the textural, physical, and chemical properties of the $Ce_{1-x}Ti_xO_2$ supports were measured and compared to $Ce_{0.5}Zr_{0.5}O_2$. It was previously established that the optimum Ce:Zr molar ratio for gold-catalyzed LTS was 1:1 (Pilasombat et al., 2012), therefore $Ce_{0.5}Zr_{0.5}O_2$ was used as the benchmark catalyst support. The bulk elemental composition of prepared supports was measured using SEM-EDX and is summarized

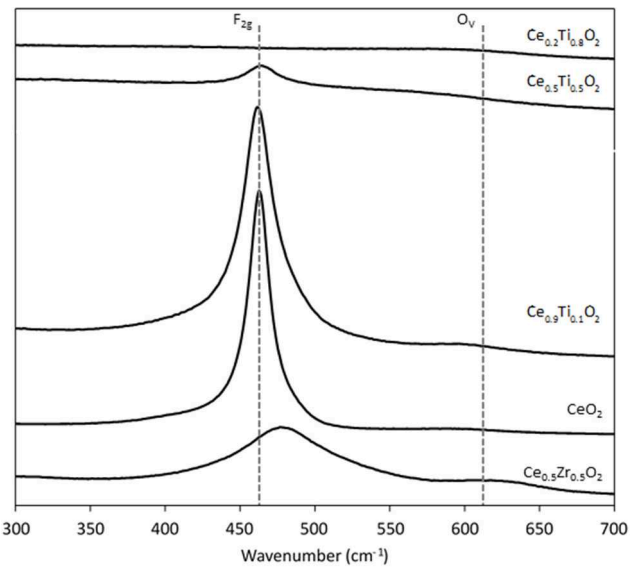

FIGURE 2 | Raman spectra of the synthesized $Ce_{0.5}Zr_{0.5}O_2$ and the $Ce_xTi_{1-x}O_2$ supports, showing the F_{2g} mode and the O_v modes.

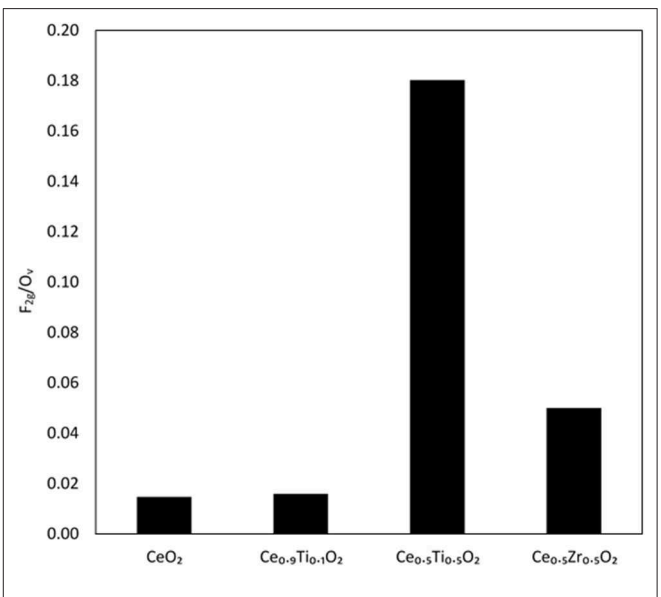

FIGURE 3 | Comparison of oxygen vacancies on Ce-based oxides as determined from Raman spectroscopy, using the ratio of the F_{2g} mode and the O_v mode.

in **Table 1**. The measured Ce:Ti ratios were close to that of the nominal values, indicating the efficacy of the preparation method. The XRD patterns are shown in **Figure 1** and feature significant differences across the range of $Ce_{1-x}Ti_xO_2$ materials prepared. CeO_2 exhibits several reflections: at 28.7, 33.2, 47.6, and 56.5°, which, respectively, correspond to the (111), (200), (220), and (311) planes of the fluorite-type cubic structure (Rico-Francés et al., 2016). These features decrease in intensity as Ti content increases, indicating a loss in the long-range order of the material, which has previously been observed and ascribed the formation of a solid solution. Specifically, $Ce_{0.9}Ti_{0.1}O_2$ and $Ce_{0.5}Ti_{0.5}O_2$ exhibited a fluorite structure, while $Ce_{0.2}Ti_{0.8}O_2$ and $Ce_{0.1}Ti_{0.9}O_2$ were amorphous. The Scherrer equation was used to estimate the crystallite size of the support materials from the most intense reflection, shown in **Table 1**. The estimated crystallite size of CeO_2 was 123 Å. The introduction of 10 mol % Ti to CeO_2 induced a reduction in the crystallite size to 50 Å. Reduced crystallite sizes were also observed in the $Ce_{0.2}Ti_{0.8}O_2$ and $Ce_{0.5}Ti_{0.5}O_2$ materials while the crystallite size of $CeZrO_4$ was estimated to be 70 Å.

N_2 physisorption was carried out to measure the specific surface area of the support materials. The BET surface area measurements are presented in **Table 1**. The specific surface area of CeO_2 was measured to be 62 $m^2\ g^{-1}$, respectively, while the mixed metal oxides all exhibited higher surface areas, consistent with the lower crystallite size determined using the Scherrer equation. The highest surface areas were observed in the amorphous materials, with $Ce_{0.2}Ti_{0.8}O_2$ exhibiting a specific surface area of 300 $m^2\ g^{-1}$ followed by $Ce_{0.1}Ti_{0.9}O_2$, which was measured to be 190 $m^2\ g^{-1}$. $Ce_{0.5}Zr_{0.5}O_2$ exhibited a surface area of 83 $m^2\ g^{-1}$, lower than the $Ce_{1-x}Ti_xO_2$ materials.

Each support was examined using Raman spectroscopy and the resulting spectra are presented in **Figure 2**. There are two main features in the prepared materials: a large band at 460 cm^{-1}, associated with the F_{2g} stretching mode of the CeO_2 fluorite structure and a weak mode at 600 cm^{-1}, denoted O_v and assigned to oxygen defects on the surface of the cubic structure of CeO_2 (Graham et al., 1991; Spanier et al., 2001; Laguna et al., 2010, 2015). The line shape and position of the F_{2g} mode varies across the $Ce_{1-x}Ti_xO_2$ supports, as previously reported. Spanier et al. reported that the size of a CeO_2 nanoparticle affected both the position of the band as well as the line shape, with smaller particles giving broader, more asymmetric bands at lower energies (Spanier et al., 2001). In addition, the intensity of the band has been shown to be proportional to the particle size of CeO_2 (Graham et al., 1991). As Ti content increases, the line shape of this Raman feature decreases in intensity and broadens, suggesting that the particle size decreased after the addition of Ti. This observation is consistent with the BET and XRD data that showed an increase in surface area and a decrease in crystallite size, respectively. The relative concentration of oxygen vacancies in each sample was calculated using a method previously described that involves the calculation of the ratio of the area of the O_v mode to the F_{2g} mode (Graham et al., 1991; Pu et al., 2007; Laguna et al., 2010). The calculated ratios are shown in **Figure 3** for the samples that exhibited an F_{2g} mode and show that an increase in Ti content leads to a significant increase in the O_v/F_{2g} ratio. $Ce_{0.5}Ti_{0.5}O_2$ exhibited the highest ratio, but $Ce_{0.2}Ti_{0.8}O_2$ did not exhibit a measurable O_v mode, therefore calculating the ratio was not possible. However, the previous textural characterization of $Ce_{0.2}Ti_{0.8}O_2$ suggests that at this high surface area, small crystallite material would possess a high number of defect sites. $Ce_{0.5}Zr_{0.5}O_2$ was included for comparison, as this material is known to have a high concentration of defects. These data demonstrate that the introduction of Ti to CeO_2 causes a large increase in the concentration of oxygen defects in the mixed metal oxides. The importance of oxygen defects in supported metal catalysts has been previously reported by Laguna et al. (2015) who showed that oxygen defect sites promote high dispersion and strong anchoring of gold on the support. In the context of the LTS reaction, the oxygen vacancies serve as activation sites for water and are therefore required in abundance for highly active LTS catalysts. The data presented in **Figure 3** indicate that $Ce_{0.5}Ti_{0.5}O_2$ (and $Ce_{0.2}Ti_{0.8}O_2$) have a higher concentration of oxygen defects than $Ce_{0.5}Zr_{0.5}O_2$, suggesting that these materials would be effective catalyst supports for the LTS reaction. Characterization of the physical and chemical properties of the mixed cerium-titanium oxides showed that high surface area materials with a high density of defect sites could be prepared using the sol-gel methodology.

Gold was deposited onto the prepared supports using a deposition-precipitation (DP) method previously reported

TABLE 2 | Analysis of the 2 wt% Au/$Ce_xTi_{1-x}O_2$ and 2 wt% Au/$Ce_{0.5}Zr_{0.5}O_2$ catalysts.

Catalyst	Metal loading[a] (%)	Ce:M molar ratio[b]	Au species composition (%)[b]			Binding energy (eV)[b]		
			Au^0	Au^{0*}	Au^{3+}	Au^0	Au^{0*}	Au^{3+}
Au/CeO_2	1.72	–	63.0	26.7	10.3	83.6	85.1	86.9
$Au/Ce_{0.9}Ti_{0.1}O_2$	1.70	10.5	68.3	10.7	21.0	84.3	85.7	86.8
$Au/Ce_{0.5}Ti_{0.5}O_2$	1.30	0.7	58.0	24.9	17.2	84.1	85.2	86.9
$Au/Ce_{0.2}Ti_{0.8}O_2$	1.08	0.9	50.6	28.2	21.1	84.1	85.2	86.9
$Au/Ce_{0.1}Ti_{0.9}O_2$	0.69	0.1	75.1	24.9	0	84.2	85.5	-
$Au/Ce_{0.5}Zr_{0.5}O_2$	1.59	1.8	61.4	20.8	17.8	84.0	85.4	86.9

[a] *Total metal loading determined using MP-AES.*

[b] *Ce:M molar ratio (where M=Ti or Zr) and Au species composition determined using XPS.*

(Carter et al., 2016). It is common for catalysts prepared using DP to have metal loadings lower than their nominal value due to the poor interaction between aqueous metal precursor and support surface that enhances metal dispersion. The actual metal loadings of the catalysts were determined using MP-AES after digestion of the catalysts in *aqua regia*. The supported metal loading is shown in **Table 2**. The measured values show that the Au loading increases with Ce content. Au/CeO_2 had a metal loading of 1.72 wt% while $Au/Ce_{0.1}Ti_{0.9}O_2$ had 0.69 wt% Au. These data indicate that the surface charge of TiO_2 is more negative at pH 8 than that of CeO_2, consistent with previously reported PZC values (De Faria and Trasatti, 1994; Kosmulski, 2002).

XPS analysis of the prepared catalysts was carried out to examine the composition of the catalyst surface. Comparison of the Ce:M molar ratio using XPS analysis allows the comparison between the surface composition and the bulk composition, determined using SEM-EDX. The values match the EDX values from **Table 1** closely, with the exception of $Ce_{0.2}Ti_{0.8}O_2$, which has a higher than expected Ce:Ti ratio from the XPS analysis. This suggests some surface enrichment of Ce in the catalyst support. The deconvoluted Au 4f spectrum of each catalyst is presented in **Figure 4**. Three distinct Au species were observed in each catalyst. In $Au/Ce_{0.5}Zr_{0.5}O_2$, these were measured to be at 84.0, 85.4 and 86.9 eV, which were assigned to Au^0, Au^{0*}, and Au^{3+}. The notation Au^{0*} refers to small metallic Au nanoparticles (i.e., below ~2 nm) and has been widely reported (Luo et al., 2001; Willneff et al., 2006; Rodriguez et al., 2014; Zhou et al., 2015; Carter et al., 2016). It was

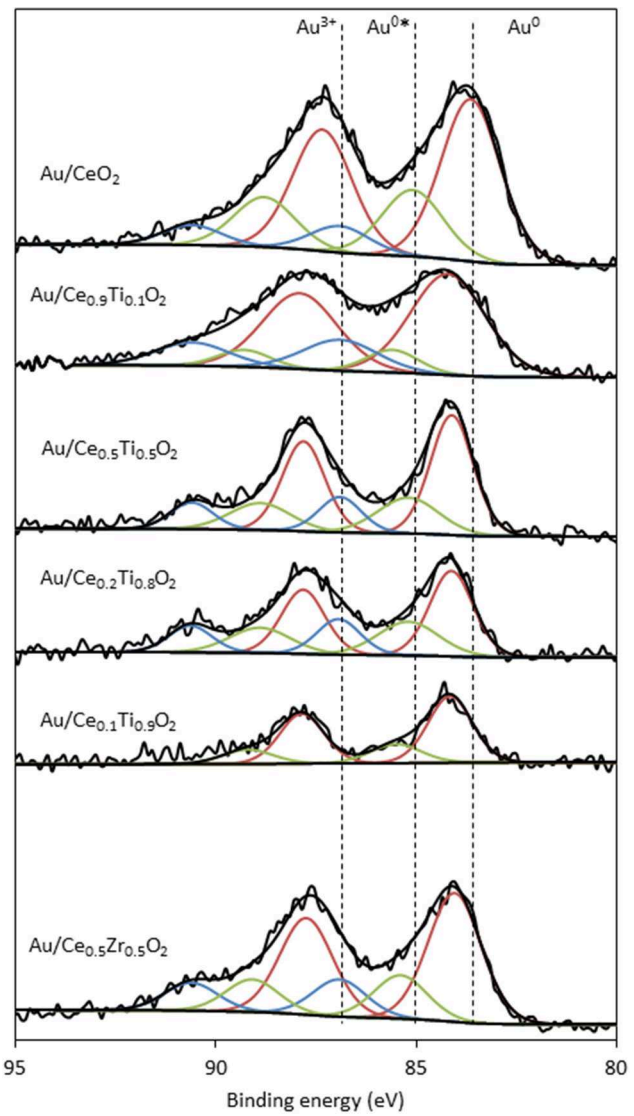

FIGURE 4 | XPS analysis of the Au 4f spectra of supported gold catalysts showing the identification of three Au species: Au^0 (red), Au^{0*} (green) and Au^{3+} (blue).

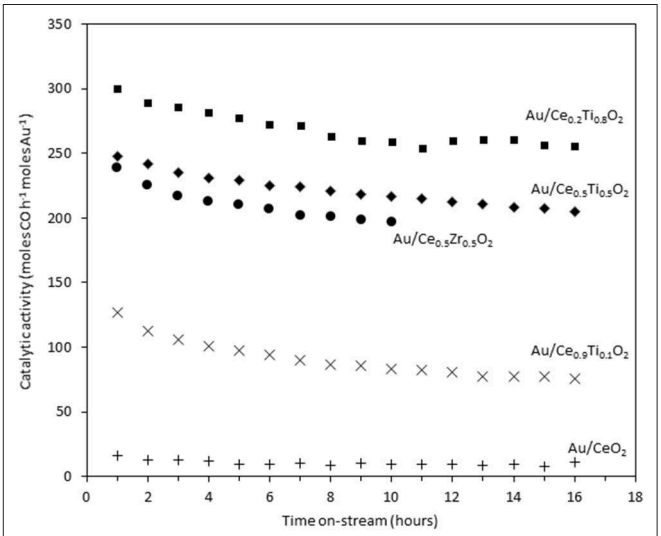

FIGURE 5 | Time on-stream activity plots for gold catalysts 10 the LTS reaction: 0.150 g catalyst, 150°C, 100 ml min^{-1}, 2% CO, 2% CO_2, 7.5% H_2O, 8.1% H_2, 80.4% N_2.

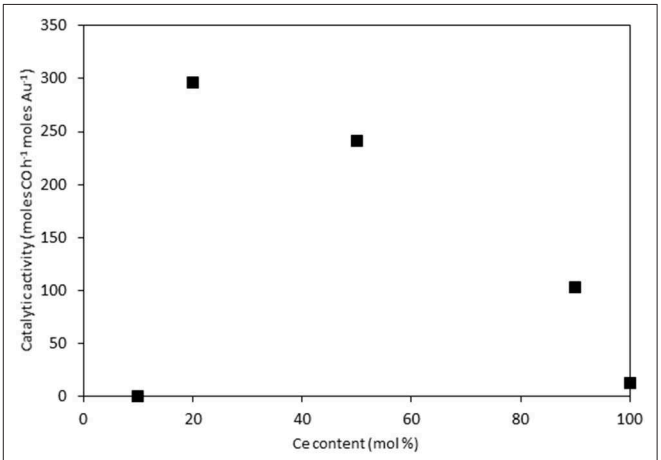

FIGURE 6 | LTS activity for $Au/Ce_xTi_{1-x}O_2$ catalysts after 90 min on-stream: 0.150 g catalyst, 150°C, 100 ml min^{-1}, 2% CO, 2% CO_2, 7.5% H_2O, 8.1% H_2, 80.4%N_2.

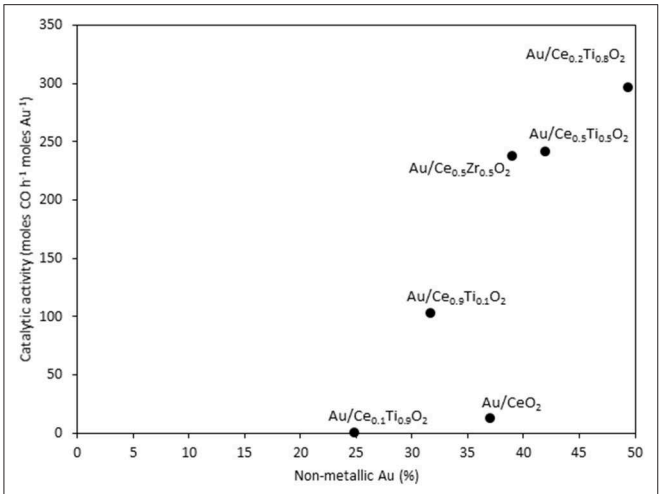

FIGURE 7 | The LTS activity after 1 h on-stream plotted against the concentration of non-metallic Au in the sample, as determined by XPS.

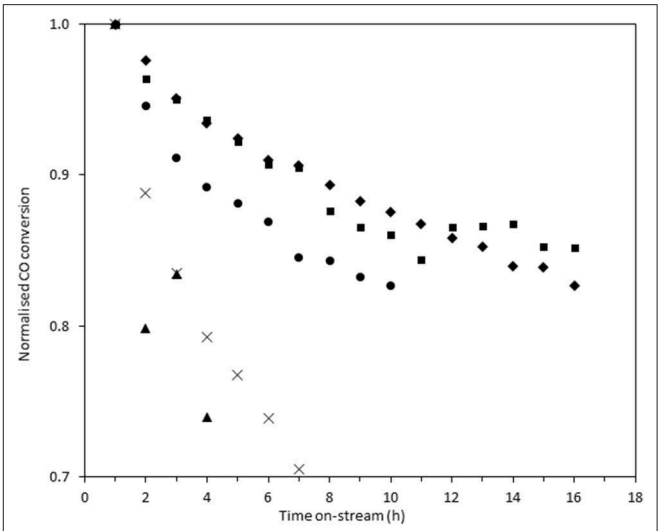

FIGURE 8 | Normalized on-stream conversion of $Au/Ce_{0.2}Ti_{0.8}O_2$ (■), $Au/Ce_{0.5}Ti_{0.5}O_2$(♦), $Au/Ce_{0.5}Zr_{0.5}O_2$ (●), $Au/Ce_{0.9}Tl_{0.1}O_2$ (×), and Au/CeO_2 (▲) in LTS reaction 0.150 g catalyst, 150°C, 100 ml min^{-1}, 2% CO, 2% CO_2, 7.5% H_2O, 8.1% H_2 80.4% N_2. Conversions were normalized against their conversion at 1 h on-stream.

also noted that the binding energy of each Au species was dependent on the composition of the support, consistent with previous investigations (Wayne Goodman, 2010). The composition of different Au species in each catalyst sample varied systematically across the sample set as shown in **Table 2**. Of particular importance are the Au^{3+} and Au^{0*} species, which were previously identified as being catalytically active or precursors to catalytically active species (Burch et al., 2010; Carter et al., 2017). $Au/Ce_{0.2}Ti_{0.8})_2$ exhibited the highest concentration of such Au species, suggesting that it would exhibit the highest LTS activity.

The catalysts were investigated for their activity in the LTS reaction 150°C. The time on-line data is shown in **Figure 5**. The units of catalytic activity are expressed as the number of moles of CO converted per hour, per mole of gold (moles CO h^{-1} moles Au^{-1}) to account for the variation in the metal loadings between each catalyst, which is shown in **Table 2**. It should be noted that the conversions reported herein are far from the thermodynamic equilibrium conversion, which was calculated to be > 99% (the most active catalysts in this work gave approximately 50% conversion). The order of activity was: $Au/Ce_{0.2}Ti_{0.8}O_2$ > $Au/Ce_{0.5}Ti_{0.5}O_2$ > $Au/Ce_{0.5}Zr_{0.5}O_2$ > $Au/Ce_{0.9}Ti_{0.1}O_2$ > Au/CeO_2. It was previously reported that $Au/Ce_{0.2}Ti_{0.8}O_2$ was more active than $Au/Ce_{0.5}Ti_{0.5}O_2$ (Manzoli et al., 2007), which is consistent with the current work and could reflect the difference in the number of active sites that can be stabilized on the mixed metal oxide at different Ce:Ti ratios. $Au/Ce_{0.1}Ti_{0.9}O_2$ did not exhibit catalytic activity. It is likely that $Au/Ce_{0.1}Ti_{0.9}O_2$ was not active for the same reason that TiO_2 is not active under similar conditions; that water cannot be efficiently activated on the surface (Tibiletti et al., 2005). $Au/Ce_{0.2}Ti_{0.8}O_2$ and $Au/Ce_{0.5}Ti_{0.5}O_2$ exhibited higher activity than the benchmark $Au/Ce_{0.5}Zr_{0.5}O_2$catalyst, demonstrating the effectiveness of ceria-titania mixed metal oxides as catalyst supports and their proficiency to stabilize small gold nanoparticles, the active species in the LTS reaction (Fu et al., 2003; Tibiletti et al., 2005). The high dispersion of Au in these catalysts is inferred from the distribution of Au species measured by XPS. The most active catalysts featured a high proportion of Au^{3+} or Au^{0*}. Comparison of the ceria-titania catalysts is shown in **Figure 6**, which plots the activity after 90 min on-stream against the Ce content (mol %) in the mixed metal oxide supports. It is clear that a combination of cerium and titanium is required for a highly active catalyst. The origin of this synergy is likely due to two properties of the support: surface area and oxygen defect density. A high surface area can enable a high dispersion of supported metal, while a high oxygen defect density gives a catalyst with many nucleation sites for gold and activation sites for water (Pojanavaraphan et al., 2013; Laguna et al., 2015). **Figure 7** shows the relationship between catalytic activity and the proportion of non-metallic Au in the sample, demonstrating a positive correlation. Au/CeO_2 is a slight outlier in this trend, but the CeO_2 support was found to have relatively few oxygen defect sites, which means the catalytic activity may be limited by the activation of water.

In order to measure the stability of the catalysts, the time on-line data was plotted as the normalized conversion, as described in the experimental section (**Figure 8**). The rate of deactivation varies significantly between the catalysts over the time period investigated. The most stable catalysts were $Au/Ce_{0.5}Ti_{0.5}O_2$ and $Au/Ce_{0.2}Ti_{0.8}O_2$, which retained 87 and 88% of their initial activity after 10 h on-stream. The benchmark catalyst, $Au/Ce_{0.5}Zr_{0.5}O_2$, retained 83% of its activity after 10 h. While these catalysts were more stable, the improvement represents a marginal increase in stability but in the case of $Au/Ce_{0.2}Ti_{0.8}O_2$, the catalyst exhibited enhanced stability in a more active form. Based on the consensus that the deactivation of $Au/Ce_{0.5}Zr_{0.5}O_2$ in the LTS reaction is due to the metal-support interaction,

the enhanced stability observed in the ceria-titania materials indicates that this interaction is stronger than in the ceria-zirconia catalyst. The origin of the stabilizing effect is likely due to the defect-rich support that efficiently stabilizes active Au species. In the case of $Ce_{0.2}Ti_{0.8}O_2$, a high population of active Au species were stabilized on the support, producing the most active and stable catalyst. These data therefore demonstrate that other Ce-based mixed metal oxides should be considered as catalyst supports and that highly defective oxidic supports can stabilize highly-dispersed metal species. High-resolution electron microscopy is typically used to image supported metal clusters and atoms, however the difficulty in obtaining sufficient mass contrast on CeO_2 based supported metal catalysts to resolve sub-nm species is well-known(Guo et al., 2016; Carter et al., 2017; Stere et al., 2017). In this case, despite using aberration-corrected scanning transmission electron microscopy, it was not possible to resolve these species. Consequently, statistically-relevant particle size distributions in the fresh and used catalysts could not be obtained.

CONCLUSIONS

A series of mixed metal oxides formed of cerium and titanium were prepared using a sol-gel methodology. These were compared to $Ce_{0.5}Zr_{0.5}O_2$, the benchmark support for gold-catalyzed LTS catalysts. The textural and chemical properties of the $Ce_xTi_{1-x}O_2$ materials were measured and it was found that the Ce:Ti ratio was a crucial factor in determining these properties. The highest surface area was displayed by amorphous $Ce_{0.2}Ti_{0.8}O_2$. After the subsequent deposition of Au onto the supports, the catalysts were characterized using XPS. The most $Au/Ce_xTi_{1-x}O_2$ catalysts showed a high abundance of Au species typically assigned to highly dispersed non-metallic gold species. During extended LTS testing, $Au/Ce_{0.2}Ti_{0.8}O_2$ and $Au/Ce_{0.5}Ti_{0.5}O_2$ exhibited higher activity and stability than $Au/Ce_{0.5}Zr_{0.5}O_2$. The enhanced activity was ascribed to the high density of oxygen vacancies present on the ceria-titania, which is known to stabilize small gold species. These findings demonstrate that improvements to catalyst stability can be made with careful consideration of the necessary properties to achieve highly dispersed, well-anchored gold species.

DATA AVAILABILITY

The datasets generated for this study are available on request to the corresponding author.

AUTHOR CONTRIBUTIONS

JC, EN, SF, SG, and GH designed the experiments. JC and PS carried out catalyst synthesis. JC carried out catalyst testing. DM carried out and analyzed XPS. JC carried out XRD, surface area measurements, MP-AES, EDX, and Raman spectroscopy. JC and GH wrote the manuscript. SG and GH directed the research.

FUNDING

The authors would like to acknowledge European Research Council grant After the Goldrush ERC-2011-AdG-291319.

REFERENCES

Burch, R., Gladden, L., and Golunski, S. (2010). Studies of precious metal catalysts in the CARMAC programme improved catalyst specificity and selectivity through a combination of chemical engineering and greater understanding of reaction mechanisms. *Platin. Met. Rev.* 54, 137–146. doi: 10.1595/147106710x501782

Carter, J. H., Althahban, S., Nowicka, E., Freakley, S. J., Morgan, D. J., Shah, P. M., et al. (2016). Synergy and anti-synergy between palladium and gold in nanoparticles dispersed on a reducible support. *ACS Catal.* 6, 6623–6633. doi: 10.1021/acscatal.6b01275

Carter, J. H., Liu, X., He, Q., Althahban, S., Nowicka, E., Freakley, S. J., et al. (2017). Activation and deactivation of gold/ceria–zirconia in the low-temperature water–gas shift reaction. *Angew. Chemie - Int. Ed.* 56, 16037–16041. doi: 10.1002/anie.201709708

De Faria, L. A., and Trasatti, S. (1994). The point of zero charge of CeO2. *J. Colloid Interf. Sci.* 167, 352–357. doi: 10.1006/jcis.1994.1370

Francisco, M. S. P., Mastelaro, V. R., Nascente, P. A. P., and Florentino, A. O. (2001). Activity and characterization by XPS, HR-TEM, Raman spectroscopy, and bet surface area of CuO/CeO_2-TiO_2 catalysts. *J. Phys. Chem. B.* 105, 10515–10522. doi: 10.1021/jp0109675

Fu, Q., Saltsburg, H., and Flytzani-Stephanopoulos, M. (2003). Active nonmetallic Au and Pt species on ceria-based water-gas shift catalysts. *Science* 301, 935–938. doi: 10.1126/science.1085721

Fu, Q., Weber, A., and Flytzani-Stephanopoulos, M. (2001). Nanostructured $Au-CeO_2$ catalysts for low-temperature water-gas shift. *Catal. Lett.* 77, 87–95. doi: 10.1023/A:1012666128812

Goguet, A., Burch, R., Chen, Y., Hardacre, C., Hu, P., Joyner, R. W., et al. (2007). Deactivation mechanism of a $Au/CeZrO_4$ catalyst during a low-temperature water gas shift reaction. *J. Phys. Chem.* 111, 16927–16933. doi: 10.1021/jp0743976

Graham, G. W., Weber, W. H., Peters, C. R., and Usmen, R. (1991). Empirical method for determining CeO2-particle size in catalysts by raman spectroscopy. *J. Catal.* 130, 310–313. doi: 10.1016/0021-9517(91)90113-I

Guo, L. W., Du, P. P., Fu, X. P., Ma, C., Zeng, J., Si, R., et al. (2016). Contributions of distinct gold species to catalytic reactivity for carbon monoxide oxidation. *Nat. Commun.* 7:13481. doi: 10.1038/ncomms13481

Kim, S. S., Lee, S. M., Won, J. M., Yang, H. J., and Hong, S. C. (2015). Effect of Ce/Ti ratio on the catalytic activity and stability of Ni/CeO_2-TiO_2 catalyst for dry reforming of methane. *Chem. Eng. J.* 280, 433–440. doi: 10.1016/j.cej.2015.06.027

Kosmulski, M. (2002). The significance of the difference in the point of zero charge between rutile and anatase. *Adv. Colloid Interf. Sci.* 99, 255–264. doi: 10.1016/S0001-8686(02)00080-5

Laguna, O. H., Pérez, A., Centeno, M. A., and Odriozola, J. A. (2015). Synergy between gold and oxygen vacancies in gold supported on Zr-doped ceria catalysts for the CO oxidation. *Appl. Catal. B Environ.* 176–177, 385–395. doi: 10.1016/j.apcatb.2015.04.019

Laguna, O. H., Romero Sarria, F., Centeno, M. A., and Odriozola, J. A. (2010). Gold supported on metal-doped ceria catalysts (M = Zr, Zn and Fe) for the preferential oxidation of CO (PROX). *J. Catal.* 276, 360–370. doi: 10.1016/j.jcat.2010.09.027

Luo, K., Kim, D. Y., and Goodman, D. W. (2001). The nucleation and growth of gold on silica. *J. Mol. Catal. A Chem.* 167, 191–198. doi: 10.1016/S1381-1169(00)00506-9.

Manzoli, M., Vindigni, F., Chiorino, A., Tabakova, T., Idakiev, V., and Boccuzzi, F. (2007). New gold catalysts supported on mixed ceria-titania oxides for water-gas shift and preferential CO oxidation reactions. *React. Kinet. Catal. Lett.* 91:213. doi: 10.1007/s11144-007-5084-6

Park, J. B., Graciani, J., Evans, J., Stacchiola, D., Ma, S., Liu, P., et al. (2009). High catalytic activity of Au/CeOx/TiO_2(110) controlled by the nature of the mixed-metal oxide at the nanometer level. *Proc. Natl. Acad. Sci. U.S.A.* 106, 4975–4980. doi: 10.1073/pnas.0812604106

Park, J. B., Graciani, J., Evans, J., Stacchiola, D., Senanayake, S. D., Barrio, L., et al. (2010). Gold, copper, and platinum nanoparticles dispersed on CeOx/TiO_2(110) surfaces: high water-gas shift activity and the nature of the mixed-metal oxide at the nanometer level. *J. Am. Chem. Soc.* 132, 356–363. doi: 10.1021/ja9087677

Pilasombat, R., Daly, H., Goguet, A., Breen, J. P., Burch, R., Hardacre, C., et al. (2012). Investigation of the effect of the preparation method on the activity and stability of Au/CeZrO 4 catalysts for the low temperature water gas shift reaction. *Catal. Today*. 180, 131–138. doi: 10.1016/j.cattod.2011.04.053

Pojanavaraphan, C., Luengnaruemitchai, A., and Gulari, E. (2013). Catalytic activity of Au-Cu/CeO_2-ZrO_2 catalysts in steam reforming of methanol. *Appl. Catal. A Gen.* 456, 135–143. doi: 10.1016/j.apcata.2013.02.010

Pu, Z. Y., Lu, J. Q., Luo, M. F., and Xie, Y. L. (2007). Study of oxygen vacancies in Ce0.9Pr0.1O 2-δ solid solution by *in situ* X-ray diffraction and *in situ* raman spectroscopy. *J. Phys. Chem. C.* 111, 18695–18702. doi: 10.1021/jp0759776

Reina, T. R., Ivanova, S., Delgado, J. J., Ivanov, I., Idakiev, V., Tabakova, T., et al. (2014). Viability of Au/CeO_2-ZnO/Al_2O_3 catalysts for pure hydrogen production by the water-gas shift reaction. *ChemCatChem* 6, 1401–1409. doi: 10.1002/cctc.201300992

Rico-Francés, S., Jardim, E. O., Wezendonk, T. A., Kapteijn, F., Gascon, J., et al. (2016). Highly dispersed Ptδ+ on TixCe(1–x)O2 as an active phase in preferential oxidation of CO. *Appl. Catal. B Environ.* 180, 169–178. doi: 10.1016/j.apcatb.2015.06.031

Rodriguez, J. A., Si, R., Evans, J., Xu, W., Hanson, J. C., Tao, J., et al. (2015). Active gold-ceria and gold-ceria/titania catalysts for CO oxidation: from single-crystal model catalysts to powder catalysts. *Catal. Today* 240, 229–235. doi: 10.1016/j.cattod.2014.06.033

Rodriguez, P., Plana, D., Fermin, D. J., and Koper, M. T. M. (2014). New insights into the catalytic activity of gold nanoparticles for CO oxidation in electrochemical media. *J. Catal.* 311, 182–189. doi: 10.1016/j.jcat.2013.11.020

Rynkowski, J., Farbotko, J., Touroude, R., and Hilaire, L. (2000). Redox behaviour of ceria-titania mixed oxides. *Appl. Catal. A Gen.* 203, 335–348. doi: 10.1016/S0926-860X(00)00497-X

Spanier, J. E., Robinson, R. D., Zhang, F., Chan, S. W., and Herman, I. P. (2001). Size-dependent properties of (formula presented) nanoparticles as studied by Raman scattering. *Phys. Rev. B - Condens. Matter Mater. Phys.* 64:245407. doi: 10.1103/PhysRevB.64.245407

Stere, C. E., Anderson, J. A., Chansai, S., Delgado, J. J., Goguet, A., Graham, W. G., et al. (2017). Non-thermal plasma activation of gold-based catalysts for low-temperature water–gas shift catalysis. *Angew. Chemie - Int. Ed.* 56, 5579–5583. doi: 10.1002/anie.201612370

Tibiletti, D., Fonseca, A. A., Burch, R., Chen, Y., Fisher, J. M., Goguet, A., et al. (2005). DFT and *in situ* EXAFS investigation of gold/ceria-zirconia low-temperature water gas shift catalysts: Identification of the nature of the active form of gold. *J. Phys. Chem. B.* 109, 22553–22559. doi: 10.1021/jp054576s

Wayne Goodman, D. (2010). "Catalysis by supported gold nanoclusters," in *Dekker Encyclopedia of Nanoscience and Nanotechnology, 2nd Edn—Six Volume Set (Print Version)* (New York, NY: Taylor & Francis). doi: 10.1201/9781439834398.ch36

Willneff, E. A., Braun, S., Rosenthal, D., Bluhm, H., Hävecker, M., Kleimenov, E., et al. (2006). Dynamic electronic structure of a Au/TiO2 catalyst under reaction conditions. *J. Am. Chem. Soc.* 128, 12052–12053. doi: 10.1021/ja062792o

Zhou, Y., Peterson, E. W., and Zhou, J. (2015). Effect of nature of ceria supports on the growth and sintering behavior of Au nanoparticles. *Catal. Today*. 240, 201–205. doi: 10.1016/j.cattod.2014.04.024

Conflict of Interest Statement: The authors declare that the research was conducted in the absence of any commercial or financial relationships that could be construed as a potential conflict of interest.